Orbital entanglement and correlation from pCCD-tailored coupled cluster wave functions ⊘

Special Collection: Special Collection in Honor of Women in Chemical Physics and Physical Chemistry

Artur Nowak ; Örs Legeza; Katharina Boguslawski ✉

Check for updates

View Online   Export Citation

Articles You May Be Interested In

Time-reversal symmetry in RDMFT and pCCD with complex-valued orbitals

J. Chem. Phys. (February 2025)

Targeting excited states in all-trans polyenes with electron-pair states

J. Chem. Phys. (December 2016)

Synergy between pair coupled cluster doubles and pair density functional theory

J. Chem. Phys. (January 2015)

Orbital entanglement and correlation from pCCD-tailored coupled cluster wave functions

View Online   Export Citation   CrossMark

Artur Nowak,[1]   Örs Legeza,[2]   and Katharina Boguslawski[1,a]

AFFILIATIONS

[1] Institute of Physics, Faculty of Physics, Astronomy and Informatics, Nicolaus Copernicus University in Toruń,
Grudziadzka 5, 87-100 Torun, Poland
[2] Strongly Correlated Systems "Lendület" Research Group, Wigner Research Center for Physics, H-1525 Budapest, Hungary

Note: This paper is part of the JCP Special Collection in Honor of Women in Chemical Physics and Physical Chemistry.
[a] Author to whom correspondence should be addressed: k.boguslawski@fizyka.umk.pl

ABSTRACT

Wave functions based on electron-pair states provide inexpensive and reliable models to describe quantum many-body problems containing strongly correlated electrons, given that broken-pair states have been appropriately accounted for by, for instance, *a posteriori* corrections. In this article, we analyze the performance of electron-pair methods in predicting orbital-based correlation spectra. We focus on the (orbital-optimized) pair-coupled cluster doubles (pCCD) ansatz with a linearized coupled-cluster (LCC) correction. Specifically, we scrutinize how orbital-based entanglement and correlation measures can be determined from a pCCD-tailored CC wave function. Furthermore, we employ the single-orbital entropy, the orbital-pair mutual information, and the eigenvalue spectra of the two-orbital reduced density matrices to benchmark the performance of the LCC correction for the one-dimensional Hubbard model with the periodic boundary condition as well as the N_2 and F_2 molecules against density matrix renormalization group reference calculations. Our study indicates that pCCD-LCC accurately reproduces the orbital-pair correlation patterns in the weak correlation limit and for molecules close to their equilibrium structure. Hence, we can conclude that pCCD-LCC predicts reliable wave functions in this regime.

I. INTRODUCTION

The compromise between the computational cost of quantum-many-body methods and their accuracy and reliability is a central issue in quantum physics and chemistry. Specifically in electronic structure theory, we require methods that allow us to efficiently describe the correlated motion of electrons. Difficulties originate from the different contributions that govern the correlated motion of electrons, commonly referred to as strong and weak correlations. Conventional methods that can model strong electron correlation are based on a multireference ansatz. Examples are the complete active space self-consistent field method,[1,2] multireference coupled cluster approaches,[3–5] the density matrix renormalization group (DMRG) algorithm,[6–18] and quantum Monte Carlo methods.[19,20] Despite their applicability to problems with strongly correlated electrons, conventional multireference methods (such as conventional multiconfigurational SCF theory) typically scale exponentially with the size of the system limiting their application to small-sized or medium-sized systems. A different group of approaches suitable for strongly correlated electrons uses electron pairs, so-called geminals, to construct the electronic wave function, which is an antisymmetric product of geminals.[21] Some well-known geminal-based methods are the antisymmetric product of strongly orthogonal geminals,[21,22] the antisymmetric product of interacting geminals,[23–35] and the antisymmetric product of one-reference orbital geminals,[36,37] also known as the pair-coupled cluster doubles (pCCD) ansatz.[38] Numerical studies suggest that geminal-based approaches can accurately model systems where strong

05 April 2025 09:22:12

correlation is important, like the one-dimensional Hubbard model[37,39] or molecules with stretched bonds,[35,38,40–46] even those containing lanthanide[47] or actinide atoms.[45,48,49] Specifically, pCCD is a good approximation to the doubly occupied configuration interaction (CI) method[50,51] and requires, however, only mean-field cost. The pCCD wave function can be written as a product of geminal creation operators $\phi_i^\dagger$ acting on the vacuum state,

$$|\text{pCCD}\rangle = \prod_{i=1}^P \phi_i^\dagger |0\rangle, \tag{1}$$

with P being the number of electron pairs and

$$\phi_i^\dagger = a_i^\dagger a_{\bar{i}}^\dagger + \sum_a^{\text{virt}} c_i^a a_a^\dagger a_{\bar{a}}^\dagger, \tag{2}$$

where the sum runs over all virtual orbitals a and $\{c_i^a\}$ are the geminal expansion coefficients. In Eq. (2), i ($\bar{i}$) indicates spin-up (spin-down) electrons. The special form of the pCCD geminal creation operator [Eq. (2)] allows us to rewrite the pCCD wave function in terms of one-particle functions using an exponential ansatz[36]

$$|\text{pCCD}\rangle = \exp\left(\sum_i^{\text{occ}} \sum_a^{\text{virt}} c_i^a a_a^\dagger a_{\bar{a}}^\dagger a_{\bar{i}} a_i\right)|\Phi_0\rangle$$
$$= \exp(\hat{T}_{\text{p}})|\Phi_0\rangle, \tag{3}$$

where $|\Phi_0\rangle$ is some independent-particle wave function, for instance, the Hartree–Fock (HF) determinant, and $\hat{T}_{\text{p}}$ is the electron-pair cluster operator. Note that the cluster operator is restricted to electron pair excitations and the coupled cluster (electron-pair) amplitudes are equivalent to the pCCD geminal coefficients. Furthermore, the first sum runs over all occupied orbitals, whose number is equivalent to the number of electron pairs. The exponential form ensures the proper (linear) scaling of the method with the number of electrons (size-extensivity). Similar to CI-type methods, size-consistency can be recovered by applying an orbital-optimization protocol.[37,38,52,53] In the case of pCCD, orbital optimization leads to localized orbitals, which are symmetry-broken.[37,38,52,53]

Like other geminal-based methods,[35,42,54–57] pCCD misses a large fraction of the weak electron correlation effects that are associated with broken-pair states. This deficiency can be depleted by considering *a posteriori* corrections that are typically applied on top of a pCCD reference function. In so-called post-pCCD methods, pCCD is combined with, for instance, single-reference and multi-reference perturbation theory,[58,59] density functional theory,[45,60,61] or (linearized) coupled cluster corrections.[42,46] While numerous numerical studies on pCCD and post-pCCD exist, which demonstrate their good performance in contrast to conventional electronic structure methods,[38,41–43,45,46,49,59,62–64] these studies mostly focus on total or relative energies and energy-derived quantities (counter-examples can be found, for instance, in Refs. 37, 39, and 48). To the best of our knowledge, an in-depth analysis of electron correlation effects in post-pCCD methods has not been presented, yet. Thus, the goal of this work is to investigate the accuracy and reliability of selected post-pCCD methods in describing electron correlation going beyond the rather oversimplified picture of energies and energy-derived quantities. For that purpose,

we will employ concepts of quantum information theory (QIT). Specifically, QIT will allow us to interpret the approximate electronic wave functions using various measures of orbital entanglement and orbital-pair correlation. In this work, we will focus on the so-called single-orbital entropy and the orbital-pair mutual information.[43,44,65–73] These orbital entanglement and correlation measures can be applied to dissect electronic wave functions[43,44,74–81] and, thus, to assess the quality of electronic structure calculations. Recently, some of us have analyzed the accuracy and reliability of the pCCD model in describing electron correlation effects using the single-orbital entropy and orbital-pair mutual information.[39] Specifically, the pCCD ansatz leads to significant over-correlation, despite providing reasonable energies. It remains uncertain whether an *a posteriori* correction is able to cure the deficiencies in electron correlation effects predicted by the pCCD approach. As a post-pCCD method, we choose the recently presented pCCD-linearized coupled-cluster (LCC) models[46] as they represent a promising alternative to conventional multi-reference electronic structure methods for both electronic ground[46] and excited states,[49,63] where they statistically outperformed conventional CC methods. Furthermore, the performance of frozen-pair CC methods and their linearized variants is generally similar, where both methodologies predict similar spectroscopic constants.[82] By scrutinizing the orbital entanglement and orbital-pair correlations predicted by pCCD-LCC, we will be able to complement previous numerical studies on the performance and reliability of the LCC corrections. Additional examples where the application of orbital entanglement and correlation is profoundly insightful are the monitoring of chemical reactions,[79,80] the identification of transition states,[79] the analysis of chemical bond orders,[43,44,76,78,83] and computational protocols aspiring black-box computational setups.[66,75,81,84,85]

This work is organized as follows. In Sec. II, we briefly discuss various LCC corrections on top of pCCD. The calculation of orbital entanglement and correlation measures for a pCCD-LCC wave function is scrutinized in Sec. III. Section IV introduces the correlation measures in terms of LCC response density matrices. The computational details are summarized in Sec. V, while the numerical results are presented in Sec. VI. Finally, we conclude in Sec. VII.

II. LCC CORRECTIONS WITH A PCCD REFERENCE FUNCTION

In pCCD-LCC methods, dynamical correlation is accounted for using a coupled cluster ansatz where the HF reference determinant is substituted by the pCCD reference function,

$$|\Psi\rangle = \exp(\hat{T})|\text{pCCD}\rangle, \tag{4}$$

where $\hat{T} = \sum_\nu t_\nu \hat{\tau}_\nu$ is some general cluster operator, that is, a sum over excitation operators $\hat{\tau}_\nu$. The electronic energy can be obtained by solving the time-independent Schrödinger equation

$$\hat{H}|\Psi\rangle = E|\Psi\rangle,$$
$$\hat{H}\exp(\hat{T})|\text{pCCD}\rangle = E\exp(\hat{T})|\text{pCCD}\rangle. \tag{5}$$

The above equation can be solved using techniques of single-reference coupled cluster theory. As we seek a linearized coupled cluster correction, we have to truncate the resulting Baker–Campbell–Hausdorff (BCH) expansion after the second term to

arrive at

$$(\hat{H} + [\hat{H}, \hat{T}])|\text{pCCD}\rangle = E|\text{pCCD}\rangle. \tag{6}$$

In pCCD-linearized coupled-cluster doubles (LCCD), the cluster operator is chosen as $\hat{T} = \hat{T}_2'$, while pCCD-linearized coupled-cluster singles and doubles (LCCSD) also accounts for single excitations, $\hat{T} = \hat{T}_1 + \hat{T}_2'$. The "$\prime$" symbol indicates that pair excitations are excluded in the cluster operator as they are already accounted for in pCCD. To stress the exclusion of electron-pair excitations in the general cluster operator $\hat{T}$, we will employ the notation $\hat{T}'$ throughout this paper. Using the relation in Eq. (3), we can rewrite Eq. (6) in terms of a single reference coupled cluster ansatz,

$$(\hat{H} + [\hat{H}, \hat{T}'])\exp(\hat{T}_{\text{P}})|\Phi_0\rangle = E\exp(\hat{T}_{\text{P}})|\Phi_0\rangle, \tag{7}$$

where $\hat{T}_{\text{P}}$ is again the electron-pair cluster operator defined in Eq. (3). We can further simplify the above equation exploiting that the cluster operators $\hat{T}'$ and $\hat{T}_{\text{P}}$ commute,

$$\left(\hat{H} + [\hat{H}, \hat{T}'] + [[\hat{H}, \hat{T}'], \hat{T}_p] \right.$$
$$\left. + [\hat{H}, \hat{T}_{\text{P}}] + \frac{1}{2}[[\hat{H}, \hat{T}_{\text{P}}], \hat{T}_{\text{P}}]\right)|\Phi_0\rangle = E|\Phi_0\rangle, \tag{8}$$

where we have explicitly included the linear and quadratic terms from the pCCD reference function (the last two terms on the left-hand-side, assuming at most double excitations in $\hat{T}'$) as the exponential ansatz of pCCD is not linearized. From Eq. (8), the working equations for the electronic energy as well as for the singles and (broken-pair) doubles amplitudes can be derived using projection techniques.[46] In the following, we will employ well-known tools of conventional CC theory. Thus, it is convenient to rewrite Eq. (8) using an exponential ansatz of the form

$$\{e^{-\hat{T}'-\hat{T}_{\text{P}}}\hat{H}e^{\hat{T}_{\text{P}}+\hat{T}'}\}_{L'}|\Phi_0\rangle = E|\Phi_0\rangle. \tag{9}$$

Curly brackets indicate that all broken-pair contributions (here, $\hat{T}_1$ and $\hat{T}_2'$ or just $\hat{T}_2'$) appear at most linear when performing the BCH expansion (also labeled with the subscript L'). Exploiting this new notation, Eqs. (8) and (9) are equivalent.

III. ORBITAL-BASED CORRELATION MEASURES

In this work, we focus on orbital-based entanglement and correlation measures. Specifically, we study the single orbital entropy and orbital-pair mutual information. The single orbital entropy quantifies the entanglement between one particular orbital and the remaining set of orbitals contained in the active orbital space and is defined as[66]

$$s_i = -\sum_{\alpha=1}^{4}\omega_{\alpha;i}\ln(\omega_{\alpha;i}), \tag{10}$$

where $\omega_{\alpha;i}$ are the eigenvalues of the one-orbital reduced density-matrix (1O-RDM) for the orbital i. Thus, the single orbital entropy of the orbital i is the von Neumann entropy of the corresponding 1O-RDM. The 1O-RDM can be calculated from the one-particle and two-particle reduced density matrices (1-RDM and 2-RDM),[43,44] γ_q^p

and Γ_{rs}^{pq}, respectively. For any wave function, where the evaluation of symmetric matrix elements is feasible, the 1-RDM and 2-RDM are defined as expectation values of the form

$$\gamma_q^p = \frac{\langle\Psi|a_p^\dagger a_q|\Psi\rangle}{\langle\Psi|\Psi\rangle} \tag{11}$$

and

$$\Gamma_{rs}^{pq} = \frac{\langle\Psi|a_p^\dagger a_q^\dagger a_s a_r|\Psi\rangle}{\langle\Psi|\Psi\rangle}. \tag{12}$$

In terms of the spin-dependent 1-RDM and 2-RDM, the 1O-RDM $\boldsymbol{\rho}_i$ is diagonal and takes over a rather simple form.[43,44] For a general wave function, it can be determined as

$$\boldsymbol{\rho}_i = \begin{pmatrix} 1 - \gamma_i^i - \gamma_i^{\bar{i}} + \Gamma_{i\bar{i}}^{i\bar{i}} & 0 & 0 & 0 \\ 0 & \gamma_i^i - \Gamma_{i\bar{i}}^{i\bar{i}} & 0 & 0 \\ 0 & 0 & \gamma_i^{\bar{i}} - \Gamma_{i\bar{i}}^{i\bar{i}} & 0 \\ 0 & 0 & 0 & \Gamma_{i\bar{i}}^{i\bar{i}} \end{pmatrix}, \tag{13}$$

where the indices i label the orbital in question and i ($\bar{i}$) indicates spin-up (spin-down) electrons. The above matrix is expressed in the basis $\{-, \uparrow, \downarrow, \uparrow\downarrow\}$, representing the four possible occupations of a (spatial) orbital. We should note that ρ_i can be further simplified for pCCD. Since the pCCD model excludes singly occupied orbitals and we have the relations $\gamma_i^i = \gamma_i^{\bar{i}} = \Gamma_{i\bar{i}}^{i\bar{i}}$, the corresponding 1O-RDM of pCCD is a 2×2 matrix represented in the basis $\{-, \uparrow\downarrow\}$,[39]

$$\boldsymbol{\rho}_i^{\text{pCCD}} = \begin{pmatrix} 1 - \gamma_i^i & 0 \\ 0 & \gamma_i^i \end{pmatrix}, \tag{14}$$

as all the remaining matrix elements sum up to zero. When the LCC corrections are applied on top of the pCCD wave function, the overall 1O-RDM will be the sum of its individual contributions,

$$\boldsymbol{\rho}_i^{\text{pCCD-LCC}} = \boldsymbol{\rho}_i^{\text{pCCD}} + \boldsymbol{\rho}_i^{\text{LCC}}, \tag{15}$$

where $\boldsymbol{\rho}_i^{\text{pCCD}}$ has to be expanded to its 4×4 analog. Therefore, the hybrid pCCD-LCC 1O-RDM $\boldsymbol{\rho}_i^{\text{pCCD-LCC}}$ is a quadratic matrix of rank 4 spanned by the basis states of the one-orbital Fock space [see also Eq. (13)].

In an analogous way, the correlation between two orbitals i, j and the remaining set of orbitals is related to the two-orbital entropy,

$$s_{i,j} = -\sum_{\alpha=1}^{16}\omega_{\alpha;i,j}\ln(\omega_{\alpha;i,j}), \tag{16}$$

where $\omega_{\alpha;i,j}$ are the eigenvalues of the two-orbital (2O-)RDM $\rho_{i,j}$. In contrast to Eq. (10), the 2O-RDM is defined in terms of basis states of a two-orbital Fock space, which contains 16 possible basis states in the case of spatial orbitals. The matrix elements of the 2O-RDM can be expressed in terms of the one-particle, two-particle, three-particle, and four-particle RDMs,[43,44] γ_q^p, Γ_{rs}^{pq}, Γ_{stu}^{pqr}, and Γ_{tuvw}^{pqrs}, respectively, with

$$\Gamma_{stu}^{pqr} = \frac{\langle \Psi | a_p^\dagger a_q^\dagger a_r^\dagger a_u a_t a_s | \Psi \rangle}{\langle \Psi | \Psi \rangle} \qquad (17)$$

and

$$\Gamma_{tuvw}^{pqrs} = \frac{\langle \Psi | a_p^\dagger a_q^\dagger a_r^\dagger a_s^\dagger a_w a_v a_u a_t | \Psi \rangle}{\langle \Psi | \Psi \rangle}. \qquad (18)$$

If the electronic wave function is an eigenfunction of $\hat{S}_z$, the 2O-RDM is block-diagonal.[76] The corresponding matrix elements in terms of the N-RDMs are summarized in Table I (see also Refs. 43, 44, and 76). As for ρ_i^{pCCD}, all singly occupied states have vanishing matrix elements and the 2O-RDM of pCCD reduces to a 4×4 matrix represented in the basis states $\{--, \updownarrow-, -\updownarrow, \updownarrow\updownarrow\}$,[39]

$$\rho_{i,j}^{\mathrm{pCCD}} = \begin{pmatrix} 1 - \gamma_i^i - \gamma_j^j + \Gamma_{ij}^{\bar{i}\bar{j}} & 0 & 0 & 0 \\ 0 & \gamma_j^j - \Gamma_{ij}^{\bar{i}\bar{j}} & \Gamma_{ii}^{\bar{j}\bar{j}} & 0 \\ 0 & \Gamma_{jj}^{\bar{i}\bar{i}} & \gamma_i^i - \Gamma_{ij}^{\bar{i}\bar{j}} & 0 \\ 0 & 0 & 0 & \Gamma_{ij}^{\bar{i}\bar{j}} \end{pmatrix}. \qquad (19)$$

The 2O-RDM $\rho_{i,j}^{\mathrm{pCCD\text{-}LCC}}$ of pCCD-LCC is again the sum of its individual contributions, summarized in Table I and Eq. (19),

$$\rho_{i,j}^{\mathrm{pCCD\text{-}LCC}} = \rho_{i,j}^{\mathrm{pCCD}} + \rho_{i,j}^{\mathrm{LCC}}. \qquad (20)$$

From s_i and $s_{i,j}$, we can determine the orbital-pair mutual information[68]

$$I_{i|j} = s_i + s_j - s_{i,j}, \qquad (21)$$

which measures the correlation between the orbital pair i and j embedded in the environment of all other active-space orbitals.

The calculation of the 1O-RDM and 2O-RDM for pCCD has been investigated in Ref. 39. In the following, we, thus, focus on how the contributions of each LCC correction to the 1O-RDM and 2O-RDM of the hybrid pCCD-LCC method can be determined.

IV. REPRESENTATION OF CORRELATION MEASURES IN TERMS OF LCC RESPONSE DENSITY MATRICES

One possibility to evaluate the 1O-RDM and 2O-RDM of pCCD-LCC is to determine the response density matrices of pCCD[39] and the LCC corrections. Specifically, the correlation contribution of the CC correction on top of the pCCD wave function can be determined from

$$(\Gamma_{t\cdots}^{p\cdots})^{\mathrm{corr}} = \langle \Phi_0 | (1 + \Lambda') \{ e^{-\hat{T}' - \hat{T}_{\mathrm{P}}} \{ \hat{a}_p^\dagger \cdots a_t \} e^{\hat{T}_{\mathrm{P}} + \hat{T}'} \}_{L'} | \Phi_0 \rangle, \qquad (22)$$

TABLE I. $\rho_{i,j}^{(2)}$ expressed in terms of N-RDMs. For restricted orbitals, the three equivalent sub-blocks are in bold and comprise the following matrix elements: (a) (2,2) to (5,5); (b) (6,6) and (7,7); (c) (12,12) to (15,15). See also Ref. 43. $(2,3) = (3,2)^\dagger = \gamma_i^j - \Gamma_{ii}^{\bar{j}i} - \Gamma_{ij}^{jj} + {}^3\Gamma_{iij}^{\bar{i}\bar{j}j}$, $(4,5) = (5,4)^\dagger = \gamma_i^j - \Gamma_{ii}^{i\bar{j}} - \Gamma_{ji}^{jj} + {}^3\Gamma_{iji}^{i\bar{i}j}$, $(6,6) = \Gamma_{ij}^{ij} - {}^3\Gamma_{iij}^{iij} - {}^3\Gamma_{ijj}^{ijj} + {}^4\Gamma_{iijj}^{iijj}$, $(7,7) = \Gamma_{\bar{i}\bar{j}}^{\bar{i}\bar{j}} - {}^3\Gamma_{\bar{i}\bar{i}\bar{j}}^{\bar{i}\bar{i}\bar{j}} - {}^3\Gamma_{\bar{i}\bar{j}\bar{j}}^{\bar{i}\bar{j}\bar{j}} + {}^4\Gamma_{\bar{i}\bar{i}\bar{j}\bar{j}}^{\bar{i}\bar{i}\bar{j}\bar{j}}$, $(8,8) = \Gamma_{i\bar{j}}^{i\bar{j}} - {}^3\Gamma_{ii\bar{j}}^{ii\bar{j}} - {}^3\Gamma_{i\bar{j}\bar{j}}^{i\bar{j}\bar{j}} + {}^4\Gamma_{ii\bar{j}\bar{j}}^{ii\bar{j}\bar{j}}$, $(8,9) = (9,8)^\dagger = \Gamma_{i\bar{j}}^{\bar{i}j} - {}^3\Gamma_{i\bar{j}i}^{\bar{i}ji}$, $(8,10) = (10,8)^\dagger = -\Gamma_{ji}^{\bar{i}j} + {}^3\Gamma_{ijj}^{\bar{i}jj}$, $(8,11) = (11,8)^\dagger = \Gamma_{ii}^{\bar{j}\bar{j}} + {}^3\Gamma_{iij}^{i\bar{j}\bar{j}}$, $(9,9) = \Gamma_{\bar{i}j}^{\bar{i}j} - {}^3\Gamma_{\bar{i}ij}^{\bar{i}ij} - {}^3\Gamma_{\bar{i}jj}^{\bar{i}jj} + {}^4\Gamma_{\bar{i}ijj}^{\bar{i}ijj}$, $(9,10) = (10,9)^\dagger = -\Gamma_{ji}^{\bar{i}j}$, $(9,11) = (11,9)^\dagger = \Gamma_{\bar{i}i}^{\bar{i}\bar{j}} - {}^3\Gamma_{\bar{i}ij}^{\bar{i}ji}$, $(10,10) = \Gamma_{\bar{i}j}^{\bar{i}j} - {}^3\Gamma_{\bar{i}ij}^{\bar{i}ij} - {}^3\Gamma_{\bar{i}jj}^{\bar{i}jj} + {}^4\Gamma_{\bar{i}ijj}^{\bar{i}ijj}$, $(10,11) = (11,10)^\dagger = -\Gamma_{ii}^{\bar{j}i} + {}^3\Gamma_{iij}^{\bar{i}jj}$, $(11,11) = \Gamma_{\bar{i}i}^{\bar{i}i} - {}^3\Gamma_{\bar{i}ij}^{\bar{i}ij} - {}^3\Gamma_{\bar{i}ij}^{\bar{i}ij} + {}^4\Gamma_{\bar{i}iij}^{\bar{i}iij}$, $(12,12) = {}^3\Gamma_{ijj}^{ijj} - {}^4\Gamma_{iijj}^{iijj}$, $(12,13) = (13,12)^\dagger = -{}^3\Gamma_{ijj}^{\bar{i}jj}$, $(13,13) = {}^3\Gamma_{ijj}^{\bar{i}jj} - {}^4\Gamma_{iijj}^{\bar{i}ijj}$, $(14,14) = {}^3\Gamma_{iij}^{\bar{i}ij} - {}^4\Gamma_{iijj}^{\bar{i}ijj}$, $(14,15) = (15,14)^\dagger = -{}^3\Gamma_{iij}^{\bar{i}ij}$, $(15,15) = {}^3\Gamma_{iij}^{\bar{i}ij} - {}^4\Gamma_{iijj}^{\bar{i}ijj}$, $(16,16) = {}^4\Gamma_{iijj}^{\bar{i}\bar{i}\bar{j}\bar{j}}$, $(1,1) = 1 - \gamma_i^i - \gamma_{\bar{i}}^{\bar{i}} - \gamma_j^j - \gamma_{\bar{j}}^{\bar{j}} + \Gamma_{ii}^{\bar{i}\bar{i}} + \Gamma_{jj}^{\bar{j}\bar{j}} + \Gamma_{ij}^{ij} + \Gamma_{ij}^{\bar{i}j} + \Gamma_{\bar{i}j}^{\bar{i}j} + \Gamma_{\bar{i}\bar{j}}^{\bar{i}\bar{j}} - {}^3\Gamma_{iij}^{iij} - {}^3\Gamma_{ijj}^{ijj} - {}^3\Gamma_{\bar{i}\bar{i}\bar{j}}^{\bar{i}\bar{i}\bar{j}} - {}^3\Gamma_{\bar{i}\bar{j}\bar{j}}^{\bar{i}\bar{j}\bar{j}} + {}^4\Gamma_{iijj}^{iijj}$, $(2,2) = \gamma_j^j - \Gamma_{ij}^{ij} - \Gamma_{\bar{i}j}^{\bar{i}j} - \Gamma_{jj}^{\bar{j}j} + {}^3\Gamma_{iij}^{iij} + {}^3\Gamma_{\bar{i}ij}^{\bar{i}ij} + {}^3\Gamma_{ijj}^{i\bar{j}j} - {}^4\Gamma_{iijj}^{i\bar{i}jj}$, $(3,3) = \gamma_i^i - \Gamma_{ii}^{\bar{i}i} - \Gamma_{ij}^{ij} - \Gamma_{i\bar{j}}^{i\bar{j}} + {}^3\Gamma_{iij}^{\bar{i}ij} + {}^3\Gamma_{iij}^{i\bar{i}j} + {}^3\Gamma_{ijj}^{ijj} - {}^4\Gamma_{iijj}^{i\bar{i}jj}$, $(4,4) = \gamma_j^{\bar{j}} - \Gamma_{ij}^{i\bar{j}} - \Gamma_{\bar{i}j}^{\bar{i}\bar{j}} - \Gamma_{jj}^{j\bar{j}} + {}^3\Gamma_{iij}^{ii\bar{j}} + {}^3\Gamma_{\bar{i}ij}^{\bar{i}i\bar{j}} + {}^3\Gamma_{ijj}^{ij\bar{j}} - {}^4\Gamma_{iijj}^{ii\bar{j}j}$, $(5,5) = \gamma_i^{\bar{i}} - \Gamma_{ij}^{\bar{i}j} - \Gamma_{\bar{i}j}^{\bar{i}\bar{j}} - \Gamma_{ii}^{i\bar{i}} + {}^3\Gamma_{iij}^{i\bar{i}j} + {}^3\Gamma_{ijj}^{i\bar{i}j} + {}^3\Gamma_{ijj}^{i\bar{i}j} - {}^4\Gamma_{iijj}^{i\bar{i}jj}$.

	$--$	$-\uparrow$	$\uparrow-$	$-\downarrow$	$\downarrow-$	$\uparrow\uparrow$	$\downarrow\downarrow$	$-\updownarrow$	$\uparrow\downarrow$	$\downarrow\uparrow$	$\updownarrow-$	$\uparrow\updownarrow$	$\updownarrow\uparrow$	$\downarrow\updownarrow$	$\updownarrow\downarrow$	$\updownarrow\updownarrow$
$--$	(1,1)	0	0	0	0	0	0	0	0	0	0	0	0	0	0	0
$-\uparrow$	0	**(2,2)**	**(2,3)**	0	0	0	0	0	0	0	0	0	0	0	0	0
$\uparrow-$	0	**(3,2)**	**(3,3)**	0	0	0	0	0	0	0	0	0	0	0	0	0
$-\downarrow$	0	0	0	**(4,4)**	**(4,5)**	0	0	0	0	0	0	0	0	0	0	0
$\downarrow-$	0	0	0	**(5,4)**	**(5,5)**	0	0	0	0	0	0	0	0	0	0	0
$\uparrow\uparrow$	0	0	0	0	0	**(6,6)**	0	0	0	0	0	0	0	0	0	0
$\downarrow\downarrow$	0	0	0	0	0	0	**(7,7)**	0	0	0	0	0	0	0	0	0
$-\updownarrow$	0	0	0	0	0	0	0	(8,8)	(8,9)	(8,10)	(8,11)	0	0	0	0	0
$\uparrow\downarrow$	0	0	0	0	0	0	0	(9,8)	(9,9)	(9,10)	(9,11)	0	0	0	0	0
$\downarrow\uparrow$	0	0	0	0	0	0	0	(10,8)	(10,9)	(10,10)	(10,11)	0	0	0	0	0
$\updownarrow-$	0	0	0	0	0	0	0	(11,8)	(11,9)	(11,10)	(11,11)	0	0	0	0	0
$\uparrow\updownarrow$	0	0	0	0	0	0	0	0	0	0	0	**(12,12)**	**(12,13)**	0	0	0
$\updownarrow\uparrow$	0	0	0	0	0	0	0	0	0	0	0	**(13,12)**	**(13,13)**	0	0	0
$\downarrow\updownarrow$	0	0	0	0	0	0	0	0	0	0	0	0	0	**(14,14)**	**(14,15)**	0
$\updownarrow\downarrow$	0	0	0	0	0	0	0	0	0	0	0	0	0	**(15,14)**	**(15,15)**	0
$\updownarrow\updownarrow$	0	0	0	0	0	0	0	0	0	0	0	0	0	0	0	(16,16)

where $\Lambda' = \Lambda_1 + \Lambda_2'$ or $\Lambda' = \Lambda_2'$, respectively, and

$$\Lambda_n' = \frac{1}{(n!)^2} \sum_{ij\cdots} \sum_{ab\cdots} {}' \lambda_{ab\cdots}^{ij\cdots} i^\dagger a j^\dagger b \cdots \qquad (23)$$

is the de-excitation operator, where all electron-pair de-excitations are to be excluded as they do not enter the LCC equations (again indicated by "$\prime$"). Note that we have written Eq. (22) using the exponential ansatz introduced in Eq. (9). When evaluating the LCC response density matrices, only terms that are at most linear in $\hat{T}_1$ and $\hat{T}_2'$ are to be considered. The total N-RDM used to construct the 1O-RDM and 2O-RDM is the sum of the reference contribution, the leading correlation contribution [Eq. (22)], and all lower-order correlation contributions,

$$\Gamma_{t\cdots}^{p\cdots} = (\Gamma_{t\cdots}^{p\cdots})^{\mathrm{ref}} + (\Gamma_{t\cdots}^{p\cdots})^{\mathrm{corr}} + \{(\Gamma_{t\cdots}^{p\cdots})_{(N-1,\cdots,1)}^{\mathrm{corr}}\}, \qquad (24)$$

where the last term indicates all possible lower-order ($N − 1, \ldots, 1$) correlation contributions to the N-RDM in question.

To evaluate the response density matrices, the $\{\lambda_{ab\cdots}^{ij\cdots}\}$ amplitudes are required, which are determined by solving the Λ equations of the LCC corrections, where the first derivative of the LCC Lagrangian,

$$\mathscr{L} = E(\lambda, t) = \langle \Phi_0 | (1 + \Lambda')\{e^{-\hat{T}' - \hat{T}_\mathrm{p}} \hat{H} e^{\hat{T}_\mathrm{p} + \hat{T}'}\}_{L'} | \Phi_0 \rangle, \qquad (25)$$

with respect to the LCC amplitudes t_ν (again excluding all electron pairs) has to vanish,

$$\begin{aligned}\frac{\partial \mathscr{L}}{\partial t_\nu} &= \frac{\partial}{\partial t_\nu} \langle \Phi_0 | (1 + \Lambda')\{e^{-\hat{T}' - \hat{T}_\mathrm{p}} \hat{H} e^{\hat{T}_\mathrm{p} + \hat{T}'}\}_{L'} | \Phi_0 \rangle \\ &= \langle \Phi_0 | (1 + \Lambda')\{e^{-\hat{T}' - \hat{T}_\mathrm{p}} [\hat{H}, \hat{\tau}_\nu] e^{\hat{T}_\mathrm{p} + \hat{T}'}\}_{L'}' | \Phi_0 \rangle \\ &= 0, \end{aligned} \qquad (26)$$

where $\hat{\tau}_\nu$ is some excitation operator associated with the CC amplitude t_ν. Due to the linear ansatz of the CC correction, the resulting Λ

equations have a particular simple form and can be solved efficiently. Specifically, the only excitation vertices that couple to $\hat{\tau}_\nu$ include $\hat{T}_\mathrm{p}$. This simplification due to the partial derivative with respect to the broken-pair amplitudes has been indicated by the superscript "$\prime$" around the curly brackets. The diagrammatic representation of the LCCD and LCCSD Λ equations of pCCD-LCCD and pCCD-LCCSD is shown in Fig. 1, while their algebraic representation is summarized in Sec. S3 in the supplementary material. We should note that we do not consider any orbital response contributions in the LCC Λ equations. Thus, the resulting N-RDMs are unrelaxed as they do not account for orbital relaxation effects. The pCCD RDMs, on the other hand, are relaxed as they are determined from an orbital-optimized pCCD reference function.

Once the Λ equations of the LCC corrections have been solved, all required elements of the 1-RDM, 2-RDM, 3-RDM, and 4-RDM can be evaluated [using Eqs. (22) and (24)]. Note that the 1O-RDM and 2O-RDM are expressed using spin-resolved N-RDMs, and thus, spin-free RDMs cannot be applied to construct the entanglement and correlation measures. This generalization does, however, not pose any difficulties even if spin-free CC calculations have been performed, where all CC amplitudes are spin-summed. When evaluating Eq. (24) or Eq. (22), we can only consider the spin-block in question (e.g., $a_{\bar{p}}^\dagger a_{\bar{p}}$) omitting the spin-summation step.

Furthermore, the resulting 1O-RDM and 2O-RDM can be simplified if restricted orbitals are used, where spin-up and spin-down electrons have a common set of spatial orbitals. The resulting 1O-RDM contains only three distinct elements (one for —, ⇈, or ↑/↓), while the 2O-RDM comprises only six distinct sub-blocks. The equivalent sub-blocks are marked in bold in Table I, while all unique elements of the pCCD-LCC 2O-RDM are summarized in Table S4 in the supplementary material. Finally, the procedure to determine the orbital entanglement and correlation measures for any pCCD-CC model is similar as scrutinized above, where the similarity transformed Hamiltonian (including the de-excitation
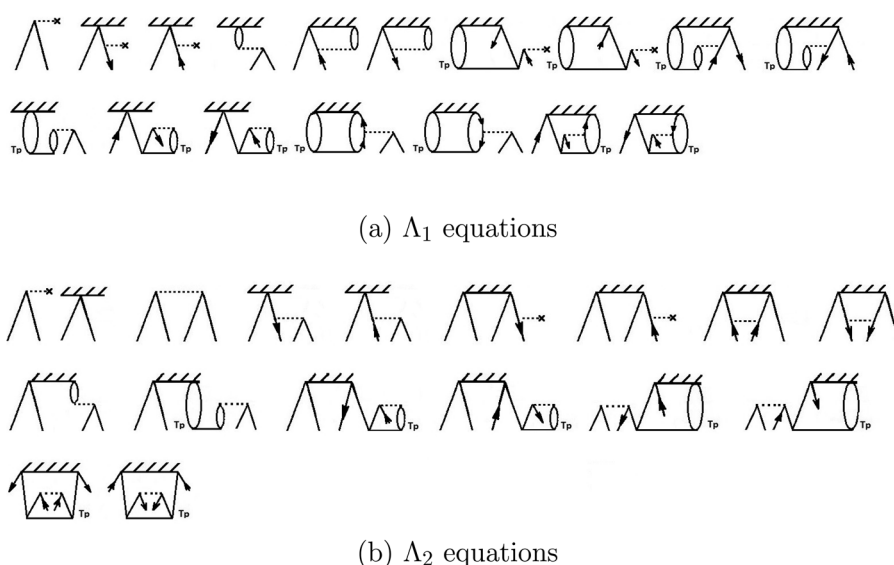

(a) Λ_1 equations

(b) Λ_2 equations

FIG. 1. Diagrammatic representation of the pCCD-LCCSD Λ equations using antisymmetrized Goldstone diagrams [second line of Eq. (26)]. $\hat{T}_\mathrm{p}$ indicates electron-pair excitation vertices. For pCCD-LCCD, the Λ_2 equations do not contain any terms comprising Λ_1 vertices.

operator, if required) has to be adjusted according to the chosen flavor of the CC correction.

V. COMPUTATIONAL DETAILS

For the investigated molecules, we employed Dunning's cc-pVDZ basis set with the following contraction: (9s, 4p, 1d) → [3s, 2p, 1d].[86]

In all pCCD calculations, we applied the variational orbital optimization protocol presented in Ref. 37 to minimize the size-consistency errors due to the stretching of molecular bonds. All pCCD-based calculations, including the orbital optimization, were performed using the PYBEST software package.[87]

As a reference, we performed DMRG calculations with the BUDAPEST QC-DMRG program.[88] The molecular orbitals obtained from the orbital-optimized pCCD calculations were chosen as the orbital basis in all DMRG calculations. The orbital ordering was optimized to enhance DMRG convergence. The minimum and the maximum number of renormalized active-system states m was varied from 256 to 1024, respectively. Finally, we also employed the dynamic block state selection (DBSS) protocol[89] to dynamically choose the number of renormalized active-system states according to a predefined threshold value for the quantum information loss. Specifically, the minimum value for m was set to 1024, the maximum value was set to 2048, while the threshold for the quantum information loss was set to 10^{-5} in all DBSS-based DMRG calculations.

VI. ORBITAL-PAIR CORRELATION SPECTRA

To benchmark orbital-pair correlations in post-pCCD wave functions, we choose three small but challenging test systems where the performance of pCCD is modest. These include systems dominated by static/nondynamic correlation (N_2), dynamical correlation (F_2), and the one-dimensional half-filled Hubbard Hamiltonian, where pCCD provides a poor reference function in the strong correlation limit.

A. The nitrogen dimer

The accurate quantum chemical description of the dissociation process of the N_2 molecule is a challenging problem for state-of-the-art computational chemistry. Specifically, along the dissociation pathway, the orbital correlation spectrum changes: while the nitrogen dimer is dominated by dynamical correlation around the equilibrium geometry, the contribution of nondynamic/static correlation significantly increases when the N–N bond is stretched. Most importantly, conventional CC methods, including pCCD-based approaches, break down in the dissociation limit, where the electronic energies diverge[42,75,81,90] (for $r_{NN} > 2.00$ Å, depending on the chosen truncated CC model). Furthermore approaching the dissociation limit, the occupied-virtual separation in pCCD breaks down, and hence, pCCD-based methods cannot properly describe the dissociation of the triple bond in the N_2 molecule.[42] This breaking point has, thus, to be visible in the correlation measures. Beyond this point, pCCD-based solutions (including the RDMs) are unphysical, and thus, accurate orbital-pair correlations cannot be determined from the CC response RDMs. To study the orbital-pair

correlation spectra along the dissociation pathway, we selected four different points along the reaction coordinate ranging from the equilibrium distance to the breaking point of pCCD-LCC. The total electronic energies determined for various quantum chemistry methods are summarized in Table S1 in the supplementary material.

Figure 2 displays the decay of the orbital-pair correlation spectra obtained for pCCD, pCCD-LCCD, pCCD-LCCSD, and DMRG at selected interatomic distances (upper panel) and the relative absolute differences in the orbital-pair mutual information with respect to the DMRG reference spectrum (lower panel). In general, the LCC correction on top of pCCD significantly improves the orbital-pair correlation spectrum at each of the selected interatomic distances (see also Figs. S1 and S10 in the supplementary material). Specifically, both pCCD-LCCD and pCCD-LCCSD accurately recover the moderate/weak orbital-pair correlations ($I_{i|j} < 10^{-1}$) around equilibrium and for a stretched N–N bond. The LCCD and LCCSD corrections, however, fail for strongly correlated orbital pairs ($I_{i|j} > 10^{-1}$), where the corresponding values of the mutual information are overestimated compared to the DMRG reference data. If we approach the breaking point of pCCD-LCC ($r_{NN} \approx 2.00$ Å), the LCC corrections overestimate all orbital-pair correlations compared to the DMRG reference spectrum as shown in Fig. 2(d). This overcorrection is also evident in the total electronic energies (see Table S1 in the supplementary material). While the differences in total energies are small around the equilibrium (around 1 mE_h), they significantly increase for a stretched N–N bond (up to 10 mE_h). The overestimation of the correlation energy can be attributed to the linearized ansatz of the CC correction.

To conclude, the LCC corrections on top of pCCD significantly improve the description of weak electron correlation effects, where the predicted values of the orbital-pair mutual information agree well with the DMRG reference (for both the equilibrium geometry and stretched bonds). Nonetheless, pCCD-LCC overestimates the dominant orbital-pair correlations along the whole dissociation pathway, which can be related to the (well-known) problem of linearized CC methods to overestimate the correlation energy.

B. The fluorine dimer

In contrast to N_2, the F_2 molecule is dominated by dynamical correlation. Furthermore, in order to describe the dissociation process of the fluorine dimer correctly, triple (or higher-order) excitations are important.[91] Conventional CC models restricted to double excitations, thus, predict spectroscopic constants of rather poor accuracy compared to more sophisticated methods and/or experimental results.[81,91] The dissociation process of the F_2 molecule, hence, represents a good test system to scrutinize orbital-pair correlations in pCCD-based methods, which are restricted to at most double excitations. As in the case of the nitrogen molecule, we focus our analysis on selected points along the potential energy surface. The corresponding energies are summarized in Table S2 in the supplementary material.

Figure 3 displays the decay of the orbital-pair correlation spectra obtained for pCCD, pCCD-LCCD, pCCD-LCCSD, and DMRG at selected interatomic distances (upper panel) and the relative absolute differences in the orbital-pair mutual information with respect to the DMRG reference spectrum (lower panel). As observed for
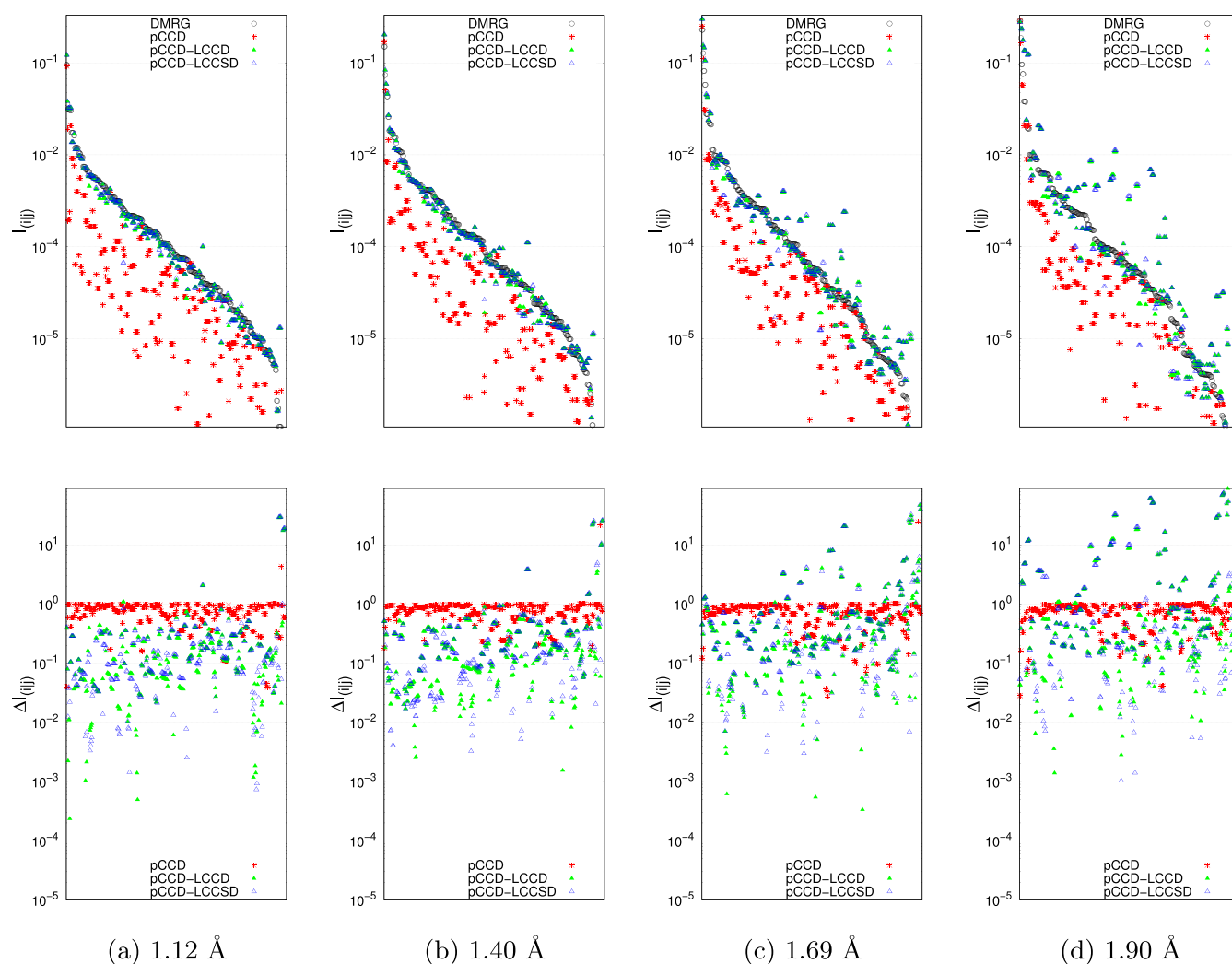
(a) 1.12 Å   (b) 1.40 Å   (c) 1.69 Å   (d) 1.90 Å

FIG. 2. Decay of the orbital-pair mutual information (upper panel) and its relative absolute difference with respect to the DMRG reference distribution (lower panel) for the N_2 molecule at different points along the reaction coordinate. The decay of the orbital-pair mutual information is sorted with respect to the DMRG reference distribution. Thus, each point $I_{i|j}$ (vertical axis) corresponds to the same orbital pair i, j (horizontal axis). The relative absolute difference is calculated as $\Delta I_{i|j} = \frac{|I_{i|j}(\text{method}) - I_{i|j}(\text{DMRG})|}{I_{i|j}(\text{DMRG})}$.

the N_2 molecule, the LCCD and LCCSD corrections on top of pCCD improve the orbital-pair correlation spectrum for each point of the reaction coordinate, where both LCC flavors recover the missing dynamical correlation effects in the pCCD reference function (see also Sec. S7 in the supplementary material, which summarizes the eigenvalue spectra of the 2O-RDM). Most importantly, the linearized CC corrections are able to capture the essential part of the dynamical correlation around equilibrium, while the leading orbital-pair correlations are slightly overestimated. However, the performance of pCCD-LCC slightly deteriorates for stretched molecular bonds. From 1.95 Å onward, the weakest orbital-pair correlations ($I_{i|j} < 10^{-4}$) are overestimated compared to the DMRG reference results. Around the equilibrium geometry as well as for stretched distances, both pCCD-LCC methods predict lower total energies than

the DMRG (differences lie between 2.00 mE_h and 9.00 mE_h, see also Table S2 in the supplementary material).

To conclude, both pCCD-LCCD and pCCD-LCCSD accurately recover the orbital-pair correlation spectrum of the F_2 molecule around equilibrium and in the vicinity of dissociation. Their performance, however, deteriorates when the F–F bond is moderately stretched. Nonetheless, the LCC corrections are able to cure some of the deficiencies of the pCCD model resulting in overall smaller relative absolute differences along the reaction coordinate.

C. The half-filled one-dimensional Hubbard Hamiltonian

Finally, we will scrutinize the orbital-pair correlation spectra of the one-dimensional (1D) Hubbard Hamiltonian[92] with periodic
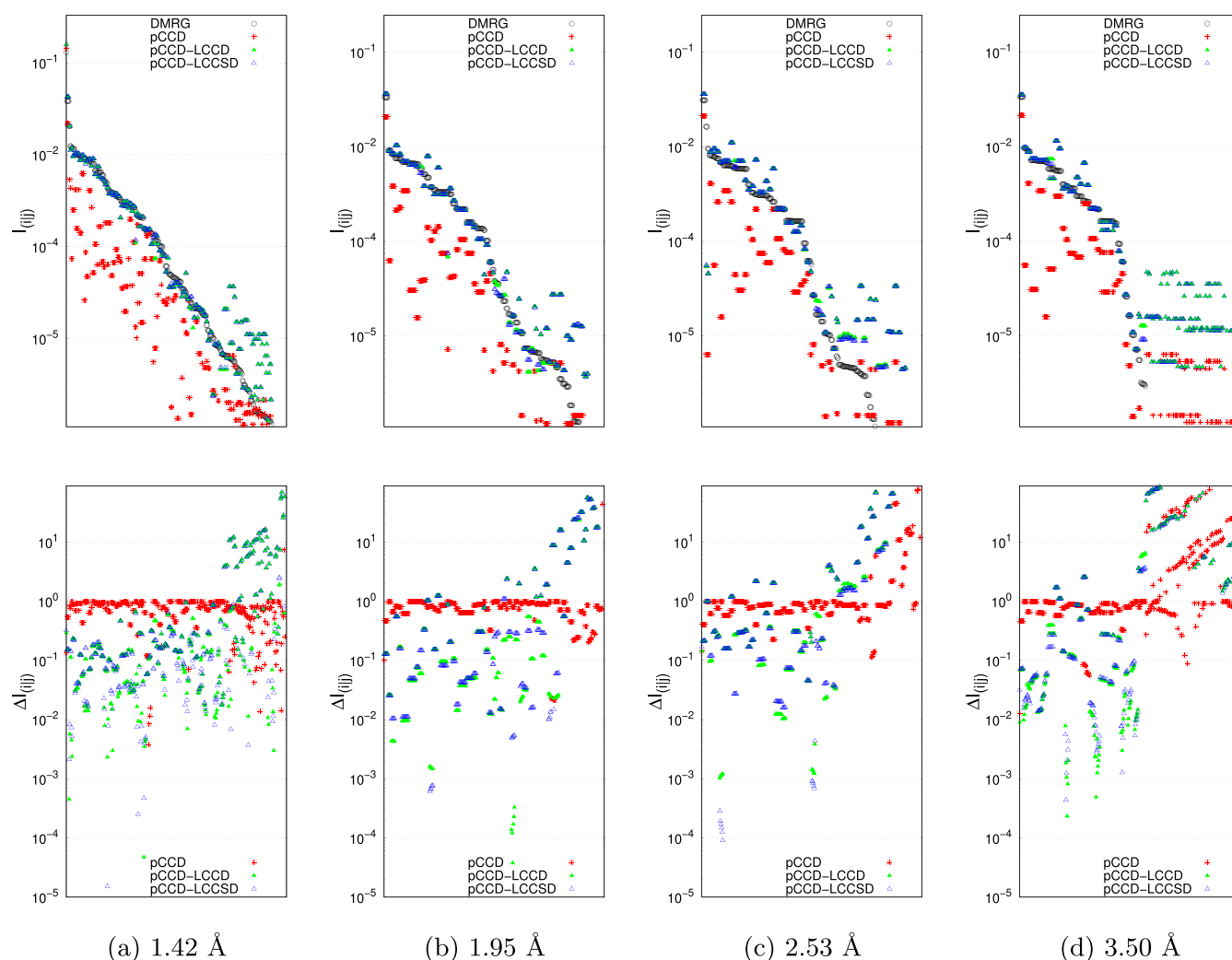
FIG. 3. Decay of the orbital-pair mutual information (upper panel) and its relative absolute difference with respect to the DMRG reference distribution (lower panel) for the F$_2$ molecule at different points along the reaction coordinate. The decay of the orbital-pair mutual information is sorted with respect to the DMRG reference distribution. Thus, each point $I_{i|j}$ (vertical axis) corresponds to the same orbital pair i, j (horizontal axis). The relative absolute difference is calculated as $\Delta I_{i|j} = \frac{|I_{i|j}(\text{method}) - I_{i|j}(\text{DMRG})|}{I_{i|j}(\text{DMRG})}$.

boundary conditions,

$$\hat{H}_{\text{Hub}} = -t \sum_{\substack{j \\ \sigma \in \{\uparrow, \downarrow\}}} \left(a_{j\sigma}^{\dagger} a_{(j+1)\sigma} + a_{(j+1)\sigma}^{\dagger} a_{j\sigma} \right) + U \sum_{j} n_{j\uparrow} n_{j\downarrow}, \quad (27)$$

where the first part describes the nearest-neighbor hopping, while the second term represents the repulsive on-site interaction, that is, $U > 0$. For the case with $U = 0\,t$ and the local site basis, the half-filled 1D Hubbard model is gapless, where all four local basis states ($|\rangle$, $|\uparrow\rangle$, $|\downarrow\rangle$, $|\uparrow\downarrow\rangle$) have equal weights of $\frac{1}{4}$ and the single-site entropy is $s_i = \ln(4)$. For increasing U/t, the charge gap opens and the weights of the unoccupied and doubly occupied basis states gradually decrease. In the limit $U/t \to \infty$, only the singly occupied states ($|\uparrow\rangle$, $|\downarrow\rangle$) have weights of $\frac{1}{2}$ resulting in a single-site entropy of $s_i = \ln(2)$

as the model becomes equivalent to the spin-$\frac{1}{2}$ Heisenberg model with an antiferromagnetic ground state. Therefore, wave functions restricted to the seniority-zero sector are not suitable to accurately describe quantum states for an increasing ratio U/t, assuming we work in the local on-site basis. The contributions of the singly occupied states can be, however, reduced if the site basis is optimized (here, within pCCD). The corresponding basis optimization results in a localized dimer basis,[37] where contributions of the unoccupied and doubly occupied states to the 1O-RDM and 2O-RDM dominate.[39] However, this localized dimer basis, which is energetically optimal for the pCCD model, yields large single-site entropies of $s_i = \ln(4)$ in the strong correlation limit. Furthermore, the single-site entropy (see also Fig. S3 in the supplementary material) exceeds the strong correlation limit of $s_i = \ln(2)$ of the on-site basis already for

$U/t \geq 4$, which highlights the strong multireference nature of the 1D Hubbard model in the pCCD dimer basis. Compared to the local on-site basis, the pCCD dimer basis will be, thus, suboptimal in the DMRG and, most likely, in post-pCCD calculations. The 1D Hubbard model, therefore, represents an ideal test case to scrutinize the performance and breaking point of post-pCCD methods.

Similar to Ref. 39, we will focus our discussion on the 1D Hubbard model with 14 sites as similar conclusions can be drawn for longer chain lengths. The total energies obtained by DMRG, pCCD, pCCD-LCCD, and pCCD-LCCSD as well as by CCD, CCSD, and their pCCD-tailored variants are summarized in Table S3 in the supplementary material. Note that only the linearized CC correction on top of pCCD could be converged for all investigated values of U/t, while the frozen-pair and conventional CC flavors suffered from convergence difficulties. As presented in Ref. 39, pCCD underestimates orbital-pair correlations for the small U/t and overestimates them starting from $U/t > 2$. In the strong correlation limit, pCCD does not provide a reliable orbital-pair correlation spectrum, where all values of the orbital-pair mutual information are overrated. Figure 4 displays the decay of the orbital-pair

correlation spectra obtained for pCCD, pCCD-LCCD, pCCD-LCCSD, and DMRG for different on-site interaction strengths (upper panel) and the relative absolute differences in the orbital-pair mutual information with respect to the DMRG reference spectrum (lower panel). In the weak correlation limit ($U/t < 2$), the LCC correction qualitatively improves the orbital-pair correlation spectra, which are similar to the DMRG reference spectrum (see also Figs. S8 and S12 in the supplementary material). Note that LCCD underestimates orbital-pair correlations, while LCCSD overestimates them compared to the DMRG reference distribution. Most importantly, the LCCSD correction breaks down for $U/t \geq 4$, where some of the eigenvalues of the 2O-RDM become negative. The reason for the breakdown of pCCD-LCCSD can be attributed to the overcorrelation in the pCCD reference function and, in conjunction with it, the large correction predicted by the LCCSD model: when combining the pCCD and LCCSD blocks in the 2O-RDM, the corresponding N-RDMs contain large negative values that overshoot the (uncorrelated, but positive) reference part. Note that the main correction to the energy originates from single excitations (or from the coupling to the single excitation manifold), and therefore,
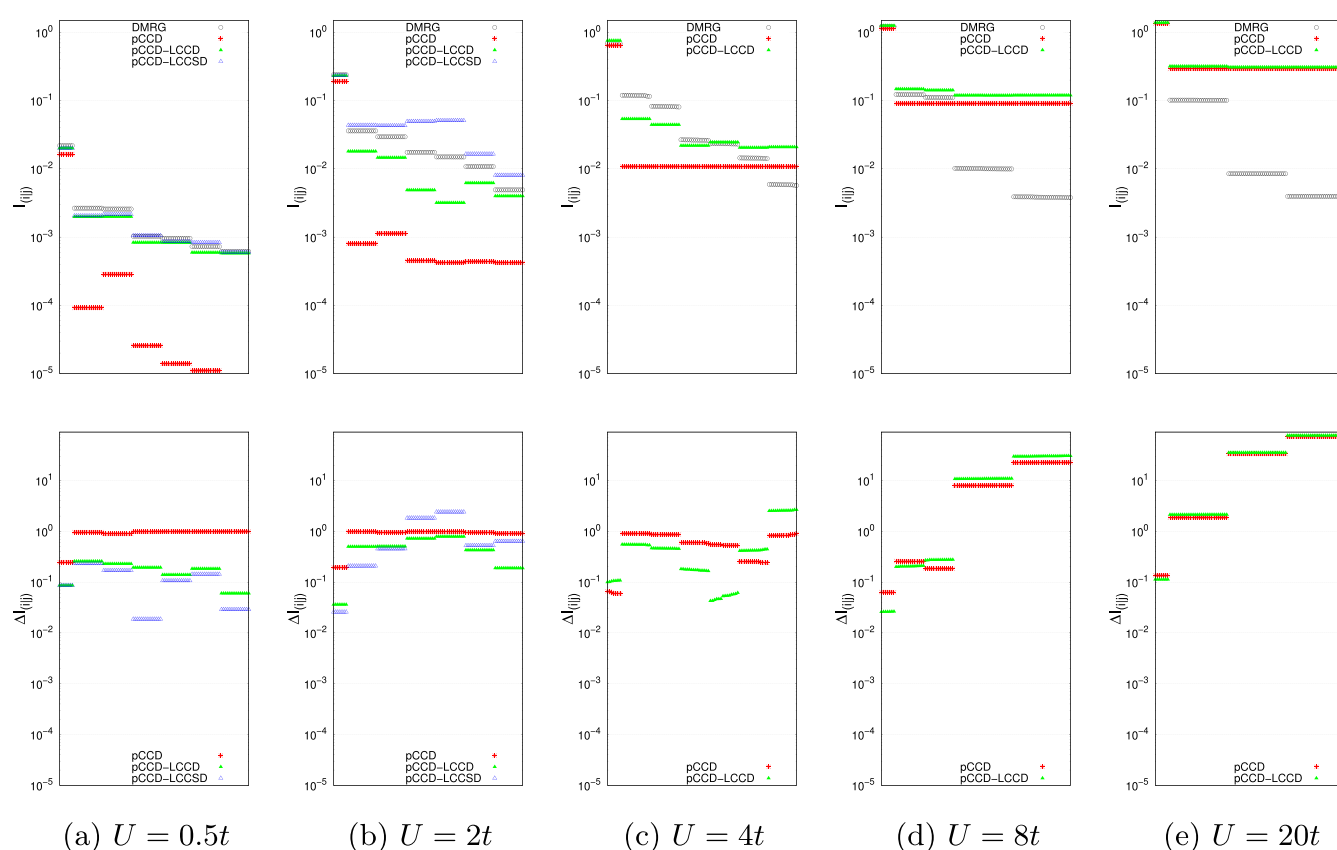

FIG. 4. Decay of the orbital-pair mutual information (upper panel) and its relative absolute difference with respect to the DMRG reference distribution (lower panel) for the half-filled Hubbard model with periodic boundary conditions for different on-site interaction strengths. The decay of orbital-pair mutual information is sorted with respect to the DMRG reference distribution. Thus, each point $I_{i|j}$ (vertical axis) corresponds to the same orbital pair i, j (horizontal axis). The relative absolute difference is calculated as $\Delta I_{i|j} = \frac{|I_{i|j}(\text{method}) - I_{i|j}(\text{DMRG})|}{I_{i|j}(\text{DMRG})}$. Note that pCCD-LCCSD does not yield a physical orbital-pair correlation spectrum for $U/t \geq 4$.

pCCD-LCCD does not break in the strong correlation limit. Thus, the corresponding LCCSD wave functions and total energies for $U/t \geq 4$ cannot be considered to be reliable, while the corresponding orbital-pair correlation spectra cannot be unambiguously determined. We should emphasize that, after the breaking point of pCCD-LCCSD ($U/t = 4$), the total electronic energies are above the exact energy and the failure of pCCD-LCCSD is only visible in the unphysical orbital-pair correlation spectra. The performance of pCCD-LCCD is more robust. Specifically, the LCCD correction provides a reliable description for the breaking point of $U/t = 4$. As expected, for larger values of U/t, the overcorrelation introduced by the pCCD reference function cannot be cured by the LCCD correction. Thus, the pCCD-LCCD correlation spectra are similar to the pCCD ones.

To conclude, although pCCD-LCC fails already for moderate values of U/t, it predicts a qualitatively correct step-decay of the orbital-pair correlation spectrum (see Fig. 4). Most importantly, a linearized CC correction on top of pCCD does provide quantitatively reliable orbital-pair correlation spectra in the weak correlation limit.

VII. CONCLUSIONS

In this work, we investigated the quality of different linearized CC corrections on top of a pCCD reference function using concepts of quantum information theory. Specifically, we derived the expressions for the 1O-RDM and 2O-RDM of pCCD-LCCD and pCCD-LCCSD in terms of their Lagrangian N-particle RDMs and scrutinized the orbital-pair correlation spectra predicted by pCCD, pCCD-LCCD, and pCCD-LCCSD. Furthermore, we compared the orbital-pair mutual information determined from pCCD-LCC to DMRG reference values (for the same molecular orbital basis). For our proof-of-principal analysis, we chose the N_2 (static/nondynamic correlation) and F_2 (dynamical correlation) di-atomic molecules and the 1D Hubbard model with periodic boundary conditions and 14 sites.

In general, the LCC corrections predict accurate and reliable orbital-pair correlation spectra around the equilibrium geometry (for molecules) or for the weak correlation limit (for the 1D Hubbard model), where the orbital-pair mutual information lies almost on top of the DMRG reference distribution. For stretched interatomic distances, pCCD-LCC methods, however, overestimate (nondynamic *and* dynamic) orbital-pair correlations. Nonetheless, the orbital-pair correlation profile predicted by both pCCD-LCCD and pCCD-LCCSD agrees with the DMRG reference distribution qualitatively, while pCCD is able to reproduce only the dominant orbital-pair correlations. On average, the values of the mutual information predicted by pCCD differ by approximately an order of magnitude from the DMRG reference values. As expected, the accuracy of the LCCD and LCCSD corrections strongly depends on the quality of the pCCD reference function, where the overcorrelation introduced by the pCCD model cannot be cured *a posteriori* as observed for the 1D Hubbard model. Most importantly, the LCCSD model on top of pCCD breaks down for $U/t \geq 4$, where the eigenvalue spectra of the 2O-RDM contain negative eigenvalues. For $U/t \geq 4$, the localized pCCD dimer basis represents a suboptimal basis for

DMRG and post-pCCD calculations as the single-site entropy features large values approaching the limit $s_i = \ln(4)$. This breakdown of pCCD-LCCSD may also be attributed to the simple response treatment of the N-RDMs, where orbital-relaxation effects have not been accounted for. Nonetheless, we do not expect that accounting for those orbital relaxation effects in the response N-RDMs will cure the failure of the pCCD-LCC description in the strong correlation regime as the overcorrelation originates from the pCCD reference function (including the optimization of the on-site basis). To conclude, the LCCD and LCCSD models can be considered reliable corrections to account for the missing correlation effects on top of a pCCD reference function at least for molecules at their equilibrium geometry or the weak correlation regime.

SUPPLEMENTARY MATERIAL

See the supplementary material for total electronic energies, the matrix representation of the 2O-RDM for pCCD-LCCSD in terms of N-particle RDMs, the algebraic form of the LCC Λ equations, the algebraic form of selected elements of the one-particle, two-particle, three-particle, and four-particle RDMs of the LCCSD correction, additional figures of the single-orbital entropy and orbital-pair mutual information, the eigenvalue spectrum of the 2O-RDM for all investigated methods, and selected error measures for the orbital-pair mutual information with respect to the DMRG reference distribution.

DATA AVAILABILITY

The data that support the findings of this study are available from the corresponding author upon reasonable request.

REFERENCES

[1] E. van Besien, K. Pierloot, and C. Görller-Walrand, "Electronic spectra of uranyl chloride complexes in acetone: A CASSCF/CASPT2 investigation," Phys. Chem. Chem. Phys. **8**, 4311 (2006).

[2] J. Paulovic, T. Nakajima, K. Hirao, and L. Seijo, J. Chem. Phys. **117**, 3597 (2002).

[3] B. Jeziorski, "Multireference coupled-cluster Ansatz," Mol. Phys. **108**, 3043–3054 (2010).

[4] D. I. Lyakh, M. Musiał, V. F. Lotrich, and R. J. Bartlett, "Multireference nature of chemistry: The coupled-cluster view," Chem. Rev. **112**, 182–243 (2012).

[5] V. V. Ivanov, D. I. Lyakh, and L. Adamowicz, "Multireference state-specific coupled-cluster methods. State-of-the-art and perspectives," Phys. Chem. Chem. Phys. **11**, 2355–2370 (2009).

[6] S. R. White, "Density matrix formulation for quantum renormalization groups," Phys. Rev. Lett. **69**, 2863–2866 (1992).

[7] S. R. White, "Density-matrix algorithms for quantum renormalization groups," Phys. Rev. B **48**, 10345–10356 (1993).

[8] S. R. White and R. L. Martin, "*Ab initio* quantum chemistry using the density matrix renormalization group," J. Chem. Phys. **110**, 4127–4130 (1999).

[9] Ö. Legeza, R. M. Noack, J. Sólyom, and L. Tincani, "Applications of quantum information in the density-matrix renormalization group," in *Computational Many-Particle Physics*, Lecture Notes Phys. Vol. 739, edited by H. Fehske, R. Schneider, and A. Weiße (Springer, Berlin/Heidelerg, 2008), pp. 653–664.

[10] K. H. Marti and M. Reiher, "The density matrix renormalization group algorithm in quantum chemistry," Z. Phys. Chem. **224**, 583–599 (2010).

[11] G. K.-L. Chan and S. Sharma, "The density matrix renormalization group in quantum chemistry," Annu. Rev. Phys. Chem. **62**, 465–481 (2011).

[12] S. Szalay, M. Pfeffer, V. Murg, G. Barcza, F. Verstraete, R. Schneider, and Ö. Legeza, "Tensor product methods and entanglement optimization for *ab initio* quantum chemistry," Int. J. Quantum Chem. **115**, 1342–1391 (2015).

[13] J. Hachmann, W. Cardoen, and G. K.-L. Chan, "Multireference correlation in long molecules with the quadratic scaling density matrix renormalization group." J. Chem. Phys. **125**, 144101 (2006).

[14] Y. Kurashige and T. Yanai, "High-performance *ab initio* density matrix renormalization group method: Applicability to large-scale multireference problems for metal compounds." J. Chem. Phys. **130**, 234114 (2009).

[15] T. Yanai, Y. Kurashige, W. Mizukami, J. Chalupský, T. N. Lan, and M. Saitow, "Density matrix renormalization group for *ab initio* calculations and associated dynamic correlation methods: A review of theory and applications," Int. J. Quantum Chem. **115**, 283–299 (2015).

[16] A. Baiardi and M. Reiher, "The density matrix renormalization group in chemistry and molecular physics: Recent developments and new challenges," J. Chem. Phys. **152**, 040903 (2020).

[17] K. Gunst, F. Verstraete, S. Wouters, Ö. Legeza, and D. Van Neck, "T3NS: Three-legged tree tensor network states," J. Chem. Theory Comput. **14**, 2026–2033 (2018).

[18] Y. Ma, S. Knecht, S. Keller, and M. Reiher, "Second-order self-consistent-field density-matrix renormalization group," J. Chem. Theory Comput. **13**, 2533–2549 (2017).

[19] S. Zhang, "Auxiliary-field quantum Monte Carlo for correlated electron systems," in *Emergent Phenomena in Correlated Matter: Autumn School Organized by the Forschungszentrum Jülich and the German Research School for Simulation Sciences at Forschungszentrum Jülich 23-27 September 2013*, Lecture Notes of the Autumn School Correlated Electrons 2013 Vol. 3 (Forschungszentrum Jülich, 2013).

[20] S. Hochkeppel, T. C. Lang, C. Brünger, F. F. Assaad, and W. Hanke, *High Performance Computing in Science and Engineering, Garching/Munich 2007: Transactions of the Third Joint HLRB and KONWIHR Status and Result Workshop, Dec. 3–4, 2007, Leibniz Supercomputing Centre, Garching/Munich, Germany* (Springer Berlin Heidelberg, Berlin, Heidelberg, 2009), Chap. Quantum Monte Carlo Studies of Strongly Correlated Electron Systems, pp. 669–686.

[21] A. C. Hurley, J. Lennard-Jones, and J. A. Pople, "The molecular orbital theory of chemical valency. XVI. A theory of paired-electrons in polyatomic molecules," Proc. R. Soc. London, Ser. A **220**, 446–455 (1953).

[22] J. M. Parks and R. G. Parr, "Theory of separated electron pairs," J. Chem. Phys. **28**, 335–345 (1958).

[23] A. J. Coleman, "Structure of fermion density matrices. II. Antisymmetrized geminal powers," J. Math. Phys. **6**, 1425–1431 (1965).

[24] S. Bratoz and P. Durand, "Transposition of the theories describing superconducting systems to molecular systems. Method for biorbitals," J. Chem. Phys. **43**, 2670–2679 (1965).

[25] D. M. Silver, "Natural orbital expansion of interacting geminals," J. Chem. Phys. **50**, 5108–5116 (1969).

[26] D. M. Silver, "Bilinear orbital expansion of geminal-product correlated wavefunctions," J. Chem. Phys. **52**, 299–303 (1970).

[27] G. Náray-Szabó, "All-pair wavefunction for many-electron states with the highest multiplicity," J. Chem. Phys. **58**, 1775–1776 (1973).

[28] G. Náray-Szabó, "All-pair wave function and reduced variational equation for electronic systems," Int. J. Qunatum Chem. **9**, 9–21 (1975).

[29] P. R. Surján, "Interaction of chemical bonds: Strictly localized wave functions in orthogonal basis," Phys. Rev. A **30**, 43–50 (1984).

[30] P. R. Surján, I. Mayer, and I. Lukovits, "Interaction of chemical bonds. II. Ab initio theory for overlap, delocalization, and dispersion interactions," Phys. Rev. A **32**, 748–755 (1985).

[31] P. R. Surján, "The interaction of chemical bonds. III. Perturbed strictly localized geminals in LMO basis," Int. J. Quantum Chem. **52**, 563–574 (1994).

[32] P. R. Surján, "The interaction of chemical bonds IV. Interbond charge transfer by a coupled-cluster-type formalism," Int. J. Quantum Chem. **55**, 109–116 (1995).

[33] P. R. Surjan, "An introduction to the theory of geminals," in *Correlation and Localization* (Springer, 1999), pp. 63–88.

[34] E. Rosta and P. R. Surján, "Interaction of chemical bonds. V. Perturbative corrections to geminal-type wave functions," Int. J. Quantum Chem. **80**, 96–104 (2000).

[35] P. R. Surján, Á. Szabados, P. Jeszenszki, and T. Zoboki, "Strongly orthogonal geminals: Size-extensive and variational reference states," J. Math. Chem. **50**, 534–551 (2012).

[36] P. A. Limacher, P. W. Ayers, P. A. Johnson, S. De Baerdemacker, D. Van Neck, and P. Bultinck, "A new mean-field method suitable for strongly correlated electrons: Computationally facile antisymmetric products of nonorthogonal geminals," J. Chem. Theory Comput. **9**, 1394–1401 (2013).

[37] K. Boguslawski, P. Tecmer, P. W. Ayers, P. Bultinck, S. De Baerdemacker, and D. Van Neck, "Efficient description of strongly correlated electrons," Phys. Rev. B **89**, 201106(R) (2014).

[38] T. Stein, T. M. Henderson, and G. E. Scuseria, "Seniority zero pair coupled cluster doubles theory," J. Chem. Phys. **140**, 214113 (2014).

[39] K. Boguslawski, P. Tecmer, and Ö. Legeza, "Analysis of two-orbital correlations in wave functions restricted to electron-pair states," Phys. Rev. B **94**, 155126 (2016).

[40] T. Zoboki, Á. Szabados, and P. R. Surján, "Linearized coupled cluster corrections to antisymmetrized product of strongly orthogonal geminals: Role of dispersive interactions," J. Chem. Theory Comput. **9**, 2602–2608 (2013).

[41] P. Tecmer, K. Boguslawski, P. A. Johnson, P. A. Limacher, M. Chan, T. Verstraelen, and P. W. Ayers, "Assessing the accuracy of new geminal-based approaches," J. Phys. Chem. A **118**, 9058–9068 (2014).

[42] T. M. Henderson, I. W. Bulik, T. Stein, and G. E. Scuseria, "Seniority-based coupled cluster theory," J. Chem. Phys. **141**, 244104 (2014).

[43] K. Boguslawski and P. Tecmer, "Orbital entanglement in quantum chemistry," Int. J. Quantum Chem. **115**, 1289–1295 (2015).

[44] K. Boguslawski and P. Tecmer, "Erratum: Orbital entanglement in quantum chemistry," Int. J. Quantum Chem. **117**, e25455 (2017).

[45] A. J. Garza, A. G. Sousa Alencar, and G. E. Scuseria, "Actinide chemistry using singlet-paired coupled cluster and its combinations with density functionals," J. Chem. Phys. **143**, 244106 (2015).

[46] K. Boguslawski and P. W. Ayers, "Linearized coupled cluster correction on the antisymmetric product of 1-reference orbital geminals," J. Chem. Theory Comput. **11**, 5252–5261 (2015).

[47] P. Tecmer, K. Boguslawski, M. Borkowski, P. S. Żuchowski, and D. Kędziera, "Modeling the electronic structures of the ground and excited states of the ytterbium atom and the ytterbium dimer: A modern quantum chemistry perspective," Int. J. Quantum Chem. **119**, e25983 (2019).

[48] P. Tecmer, K. Boguslawski, and P. W. Ayers, "Singlet ground state actinide chemistry with geminals," Phys. Chem. Chem. Phys. **17**, 14427–14436 (2015).

[49] A. Nowak, P. Tecmer, and K. Boguslawski, "Assessing the accuracy of simplified coupled cluster methods for electronic excited states in f0 actinide compounds," Phys. Chem. Chem. Phys. **21**, 19039–19053 (2019).

[50] F. Weinhold and E. B. Wilson, Jr., "Reduced density matrices of atoms and molecules. I. The 2 matrix of double-occupancy, configuration-interaction wavefunctions for singlet states," J. Chem. Phys. **46**, 2752–2758 (1967).

05 April 2025 09:22:12

[51] A. Veillard and E. Clementi, "Complete multi-configuration self-consistent field theory," Theor. Chim. Acta **7**, 133–143 (1967).

[52] K. Boguslawski, P. Tecmer, P. A. Limacher, P. A. Johnson, P. W. Ayers, P. Bultinck, S. De Baerdemacker, and D. Van Neck, "Projected seniority-two orbital optimization of the antisymmetric product of one-reference orbital geminal," J. Chem. Phys. **140**, 214114 (2014).

[53] K. Boguslawski, P. Tecmer, P. Bultinck, S. De Baerdemacker, D. Van Neck, and P. W. Ayers, "Non-variational orbital optimization techniques for the AP1roG wave function," J. Chem. Theory Comput. **10**, 4873–4882 (2014).

[54] K. Pernal, "Intergeminal correction to the antisymmetrized product of strongly orthogonal geminals derived from the extended random phase approximation," J. Chem. Theory Comput. **10**, 4332–4341 (2014).

[55] P. Jeszenszki, P. R. Nagy, T. Zoboki, Á. Szabados, and P. R. Surján, "Perspectives of APSG-based multireference perturbation theories," Int. J. Quantum Chem. **114**, 1048–1052 (2014).

[56] J. K. Ellis, R. L. Martin, and G. E. Scuseria, "On pair functions for strong correlations," J. Chem. Theory Comput. **9**, 2857–2869 (2013).

[57] V. A. Rassolov, "A geminal model chemistry," J. Chem. Phys. **117**, 5978–5987 (2002).

[58] P. A. Limacher, P. W. Ayers, P. A. Johnson, S. De Baerdemacker, D. V. Neck, and P. Bultinck, "Simple and inexpensive perturbative correction schemes for antisymmetric products of nonorthogonal geminals," Phys. Chem. Chem. Phys. **16**, 5061–5065 (2014).

[59] K. Boguslawski and P. Tecmer, "Benchmark of dynamic electron correlation models for seniority-zero wave functions and their application to thermochemistry," J. Chem. Theory Comput. **13**, 5966–5983 (2017).

[60] A. J. Garza, I. W. Bulik, T. M. Henderson, and G. E. Scuseria, "Range separated hybrids of pair coupled cluster doubles and density functionals," Phys. Chem. Chem. Phys. **17**, 22412–22422 (2015).

[61] A. J. Garza, I. W. Bulik, T. M. Henderson, and G. E. Scuseria, "Synergy between pair coupled cluster doubles and pair density functional theory," J. Chem. Phys. **142**, 044109 (2015).

[62] K. Boguslawski, "Erratum: 'Targeting excited states in all-trans polyenes with electron-pair states' [J. Chem. Phys. 145, 234105 (2016)]," J. Chem. Phys. **147**, 139901 (2017).

[63] K. Boguslawski, "Targeting doubly excited states with equation of motion coupled cluster theory restricted to double excitations," J. Chem. Theory Comput. **15**, 18–24 (2019).

[64] F. Brzęk, K. Boguslawski, P. Tecmer, and P. S. Żuchowski, "Benchmarking the accuracy of seniority-zero wave function methods for noncovalent interactions," J. Chem. Theory Comput. **15**, 4021–4035 (2019).

[65] P. Ziesche, "Correlation strength and information entropy," Int. J. Quantum Chem. **56**, 363–369 (1995).

[66] Ö. Legeza and J. Sólyom, "Optimizing the density-matrix renormalization group method using quantum information entropy," Phys. Rev. B **68**, 195116 (2003).

[67] Ö. Legeza and J. Sólyom, "Two-site entropy and quantum phase transitions in low-dimensional models," Phys. Rev. Lett. **96**, 116401 (2006).

[68] J. Rissler, R. M. Noack, and S. R. White, "Measuring orbital interaction using quantum information theory," Chem. Phys. **323**, 519–531 (2006).

[69] L. Ding, S. Mardazad, S. Das, S. Szalay, U. Schollwöck, Z. Zimborás, and C. Schilling, "Concept of orbital entanglement and correlation in quantum chemistry," J. Chem. Theory Comput. **17**, 79–95 (2021).

[70] C. Schilling and R. Schilling, "Number-parity effect for confined fermions in one dimension," Phys. Rev. A **93**, 021601 (2016).

[71] V. Vedral, "Quantum entanglement," Nat. Phys. **10**, 256–258 (2014).

[72] C. Schilling, "The quantum marginal problem," in *Mathematical Results in Quantum Mechanics* (World Scientific Publishing Company, 2014), pp. 165–176; arXiv:1404.1085.

[73] L. Ding and C. Schilling, "Correlation paradox of the dissociation limit: Formal discussion and quantitative resolution based on quantum information theory," J. Chem. Theory Comput. **16**, 4159–4175 (2020).

[74] G. Barcza, Ö. Legeza, K. H. Marti, and M. Reiher, "Quantum-information analysis of electronic states of different molecular structures," Phys. Rev. A **83**, 012508 (2011).

[75] K. Boguslawski, P. Tecmer, Ö. Legeza, and M. Reiher, "Entanglement measures for single- and multireference correlation effects," J. Phys. Chem. Lett. **3**, 3129–3135 (2012).

[76] K. Boguslawski, P. Tecmer, G. Barcza, Ö. Legeza, and M. Reiher, "Orbital entanglement in bond-formation processes," J. Chem. Theory Comput. **9**, 2959–2973 (2013).

[77] P. Tecmer, K. Boguslawski, Ö. Legeza, and M. Reiher, "Unravelling the quantum-entanglement effect of noble gas coordination on the spin ground state of CUO," Phys. Chem. Chem. Phys. **16**, 719–727 (2014).

[78] M. Mottet, P. Tecmer, K. Boguslawski, Ö. Legeza, and M. Reiher, "Quantum entanglement in carbon–carbon, carbon–phosphorus and silicon–silicon bonds," Phys. Chem. Chem. Phys. **16**, 8872–8880 (2014).

[79] C. Duperrouzel, P. Tecmer, K. Boguslawski, G. Barcza, Ö. Legeza, and P. W. Ayers, "A quantum informational approach for dissecting chemical reactions," Chem. Phys. Lett. **621**, 160–164 (2015).

[80] Y. Zhao, K. Boguslawski, P. Tecmer, C. Duperrouzel, G. Barcza, Ö. Legeza, and P. W. Ayers, "Dissecting the bond-formation process of d^{10}-metal–ethene complexes with multireference approaches," Theor. Chem. Acc. **134**, 120 (2015).

[81] K. Boguslawski, F. Réal, P. Tecmer, C. Duperrouzel, A. S. P. Gomes, Ö. Legeza, P. W. Ayers, and V. Vallet, "On the multi-reference nature of plutonium oxides: PuO_2^{2+}, PuO_2, PuO_3 and $PuO_2(OH)_2$," Phys. Chem. Chem. Phys. **19**, 4317–4329 (2017).

[82] A. Leszczyk, Ö. Legeza, M. Máté, and K. Boguslawski, "Assessing the accuracy of tailored coupled cluster methods corrected by electronic wave functions of polynomial cost" (unpublished) (2021).

[83] S. Szalay, G. Barcza, T. Szilvási, L. Veis, and Ö. Legeza, "The correlation theory of the chemical bond," Sci. Rep. **7**, 2237 (2017).

[84] C. J. Stein and M. Reiher, "Automated selection of active orbital spaces," J. Chem. Theory Comput. **12**, 1760–1771 (2016).

[85] C. J. Stein and M. Reiher, "autoCAS: A program for fully automated multiconfigurational calculations," J. Comput. Chem. **40**, 2216–2226 (2019).

[86] T. H. Dunning, Jr., "Gaussian basis sets for use in correlated molecular calculations. I. The atoms boron through neon and hydrogen," J. Chem. Phys. **90**, 1007–1023 (1989).

[87] F. Brzęk, A. Leszczyk, A. Nowak, K. Boguslawski, D. Kędziera, P. Tecmer, and P. S. Żuchowski (2020). "PyBESTv.1.0.0 (version v1.0.0)," Zenodo. https://doi.org/10.5281/zenodo.3925278

[88] Ö. Legeza, L. Veis, and T. Mosoni, QC-DMRG-Budapest, a Program for Quantum Chemical DMRG Calculations. Copyright 2000–2020, HAS RISSPO Budapest.

[89] Ö. Legeza and J. Sólyom, "Quantum data compression, quantum information generation, and the density-matrix renormalization-group method," Phys. Rev. B **70**, 205118 (2004).

[90] G. K.-L. Chan, M. Kállay, and J. Gauss, "State-of-the-art density matrix renormalization group and coupled cluster theory studies of the nitrogen binding curve," J. Chem. Phys. **121**, 6110–6116 (2004).

[91] K. Kowalski and P. Piecuch, "A comparison of the renormalized and active-space coupled-cluster methods: Potential energy curves of BH and F_2," Chem. Phys. Lett. **344**, 165–175 (2001).

[92] J. Hubbard, "Electron correlations in narrow energy bands," Proc. R. Soc. London, Ser. A **276**, 238–257 (1963).